Supplement of Atmos. Chem. Phys., 19, 921–940, 2019
https://doi.org/10.5194/acp-19-921-2019-supplement

Atmospheric Chemistry and Physics
Open Access
EGU

Supplement of

The influence of mixing on the stratospheric age of air changes in the 21st century

Roland Eichinger et al.

Correspondence to: Roland Eichinger (roland.eichinger@dlr.de)

1 Introduction

This supplement contains additional material to the article *"The influence of mixing on the stratospheric age of air changes in the 21st century"*. We provide additional figures for Sect. 3.4 of the paper. In the main article, the multi-model-means of the zonal wind $\overline{u}$, the Eliassen-Palm flux divergence, the meridonal residual circulation v^*, the meridional PV-gradient ($\partial PV/\partial y$), the diffusivity coefficient K_{yy} and the ratio $K_{yy}/|v^*|$ of eight model simulations are presented. Here, we show these quantities for each of the eight CCMI-1 (Chemistry Climate Model Intercomparison project) REF-C2 model simulations individually. The models that were used in this analysis are ACCESS, CMAM, EMAC-L47, EMAC-L90, GEOSCCM, MRI, NIWA-UKCA and WACCM. For more information on these models, the simulation setup and the selection of the models, see main article.

2 Additional figures

ACCESS

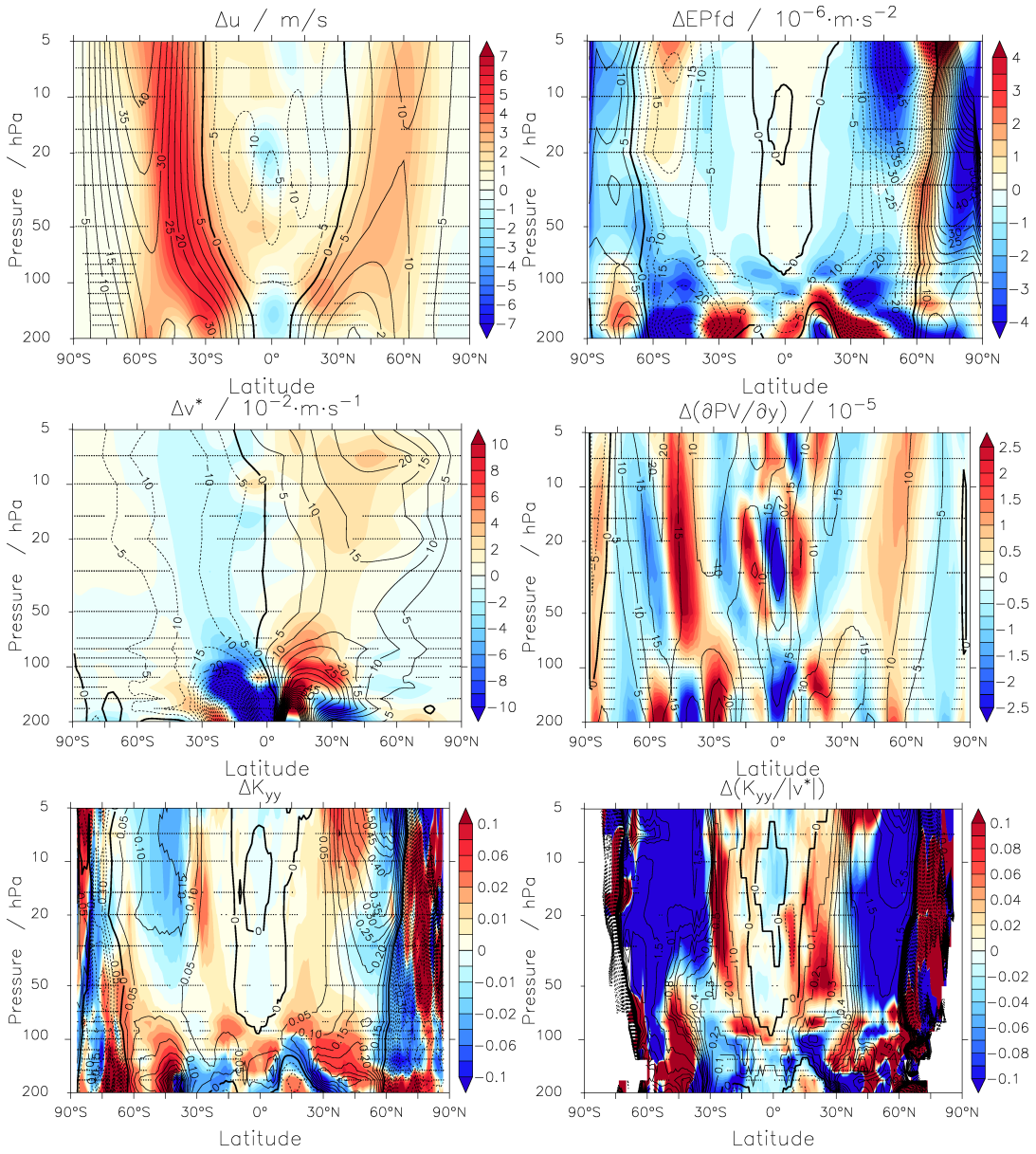

Figure 1. ACCESS CCMI REF-C2 model simulation differences (Δ) of (a) the zonal wind $\overline{u}$, (b) the EP flux divergence, (c) the meridonal residual circulation v*, (d) the meridional PV-gradient ($\partial PV/\partial y$), (e) the diffusivity coefficient K_{yy} and (f) the ratio $K_{yy}/|v^*|$ between the periods 1970-1990 and 2080-2100. The contour lines show the multi-model mean climatology of the first period of the respective quantity. Stippled regions show where the statistical significance of the difference is below the threshold 95%.

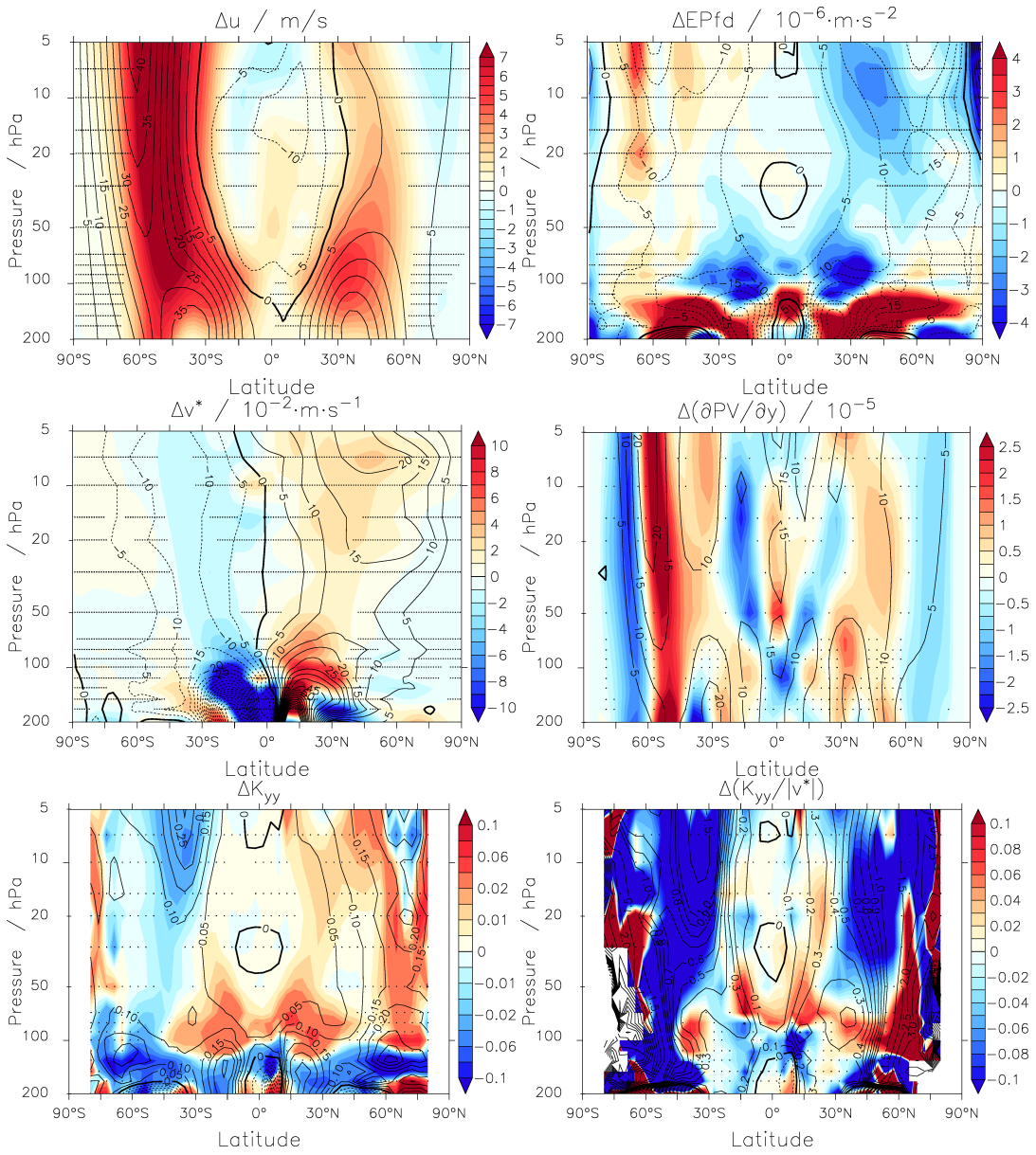

Figure 2. CMAM CCMI REF-C2 model simulation differences (Δ) of (a) the zonal wind $\overline{u}$, (b) the EP flux divergence, (c) the meridonal residual circulation v*, (d) the meridional PV-gradient ($\partial PV/\partial y$), (e) the diffusivity coefficient K_{yy} and (f) the ratio $K_{yy}/|v^*|$ between the periods 1970-1990 and 2080-2100. The contour lines show the multi-model mean climatology of the first period of the respective quantity. Stippled regions show where the statistical significance of the difference is below the threshold 95%.

EMAC-L47

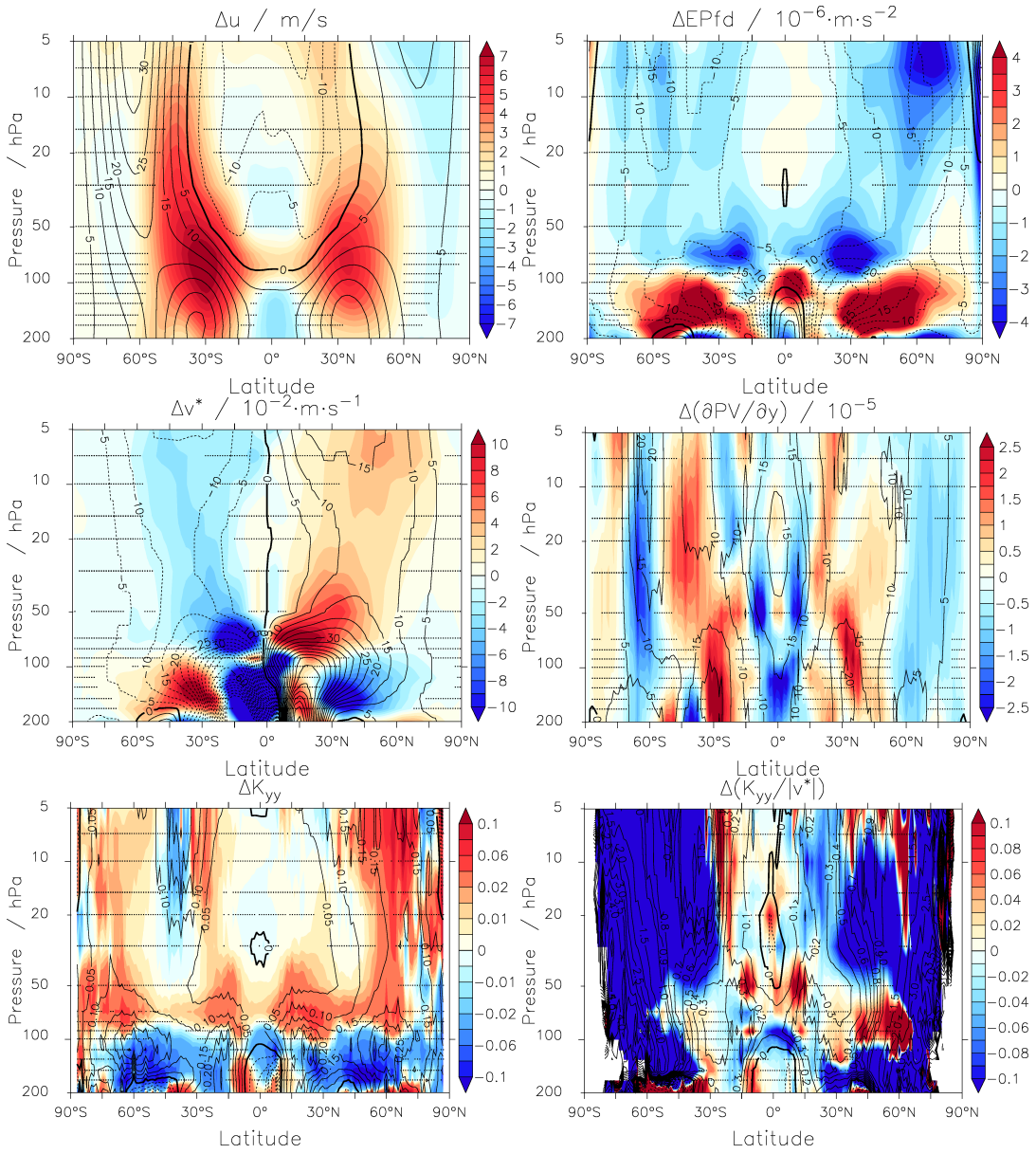

Figure 3. EMAC-L47 CCMI REF-C2 model simulation differences (Δ) of (a) the zonal wind $\overline{u}$, (b) the EP flux divergence, (c) the meridonal residual circulation v^*, (d) the meridional PV-gradient ($\partial PV/\partial y$), (e) the diffusivity coefficient K_{yy} and (f) the ratio $K_{yy}/|v^*|$ between the periods 1970-1990 and 2080-2100. The contour lines show the multi-model mean climatology of the first period of the respective quantity. Stippled regions show where the statistical significance of the difference is below the threshold 95%.

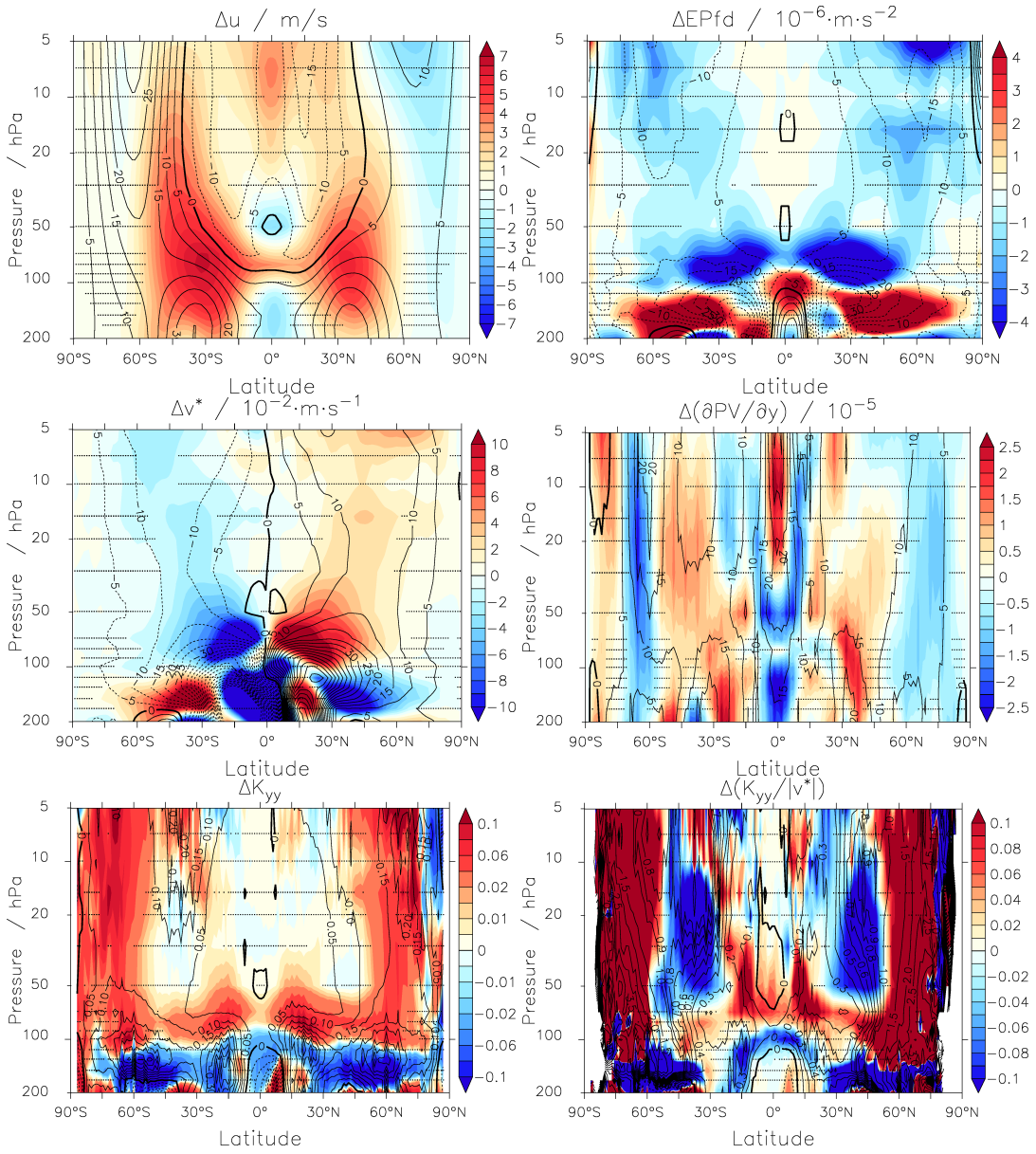

Figure 4. EMAC-L90 CCMI REF-C2 model simulation differences (Δ) of (a) the zonal wind $\overline{u}$, (b) the EP flux divergence, (c) the meridonal residual circulation v^*, (d) the meridional PV-gradient ($\partial PV/\partial y$), (e) the diffusivity coefficient K_{yy} and (f) the ratio $K_{yy}/|v^*|$ between the periods 1970-1990 and 2080-2100. The contour lines show the multi-model mean climatology of the first period of the respective quantity. Stippled regions show where the statistical significance of the difference is below the threshold 95%.

GEOSCCM

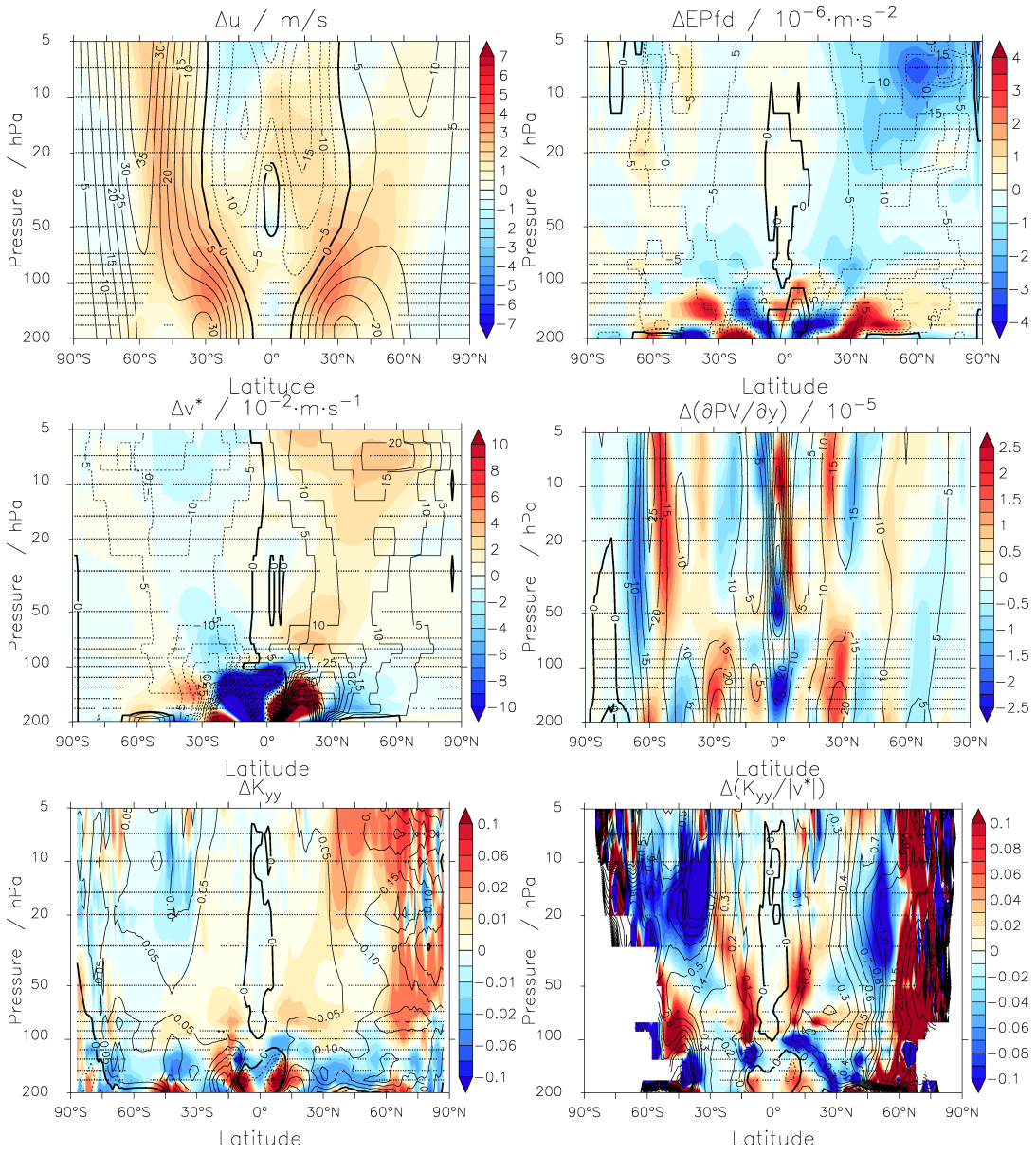

Figure 5. GEOSCCM CCMI REF-C2 model simulation differences (Δ) of (a) the zonal wind $\overline{u}$, (b) the EP flux divergence, (c) the meridonal residual circulation v*, (d) the meridional PV-gradient ($\partial PV/\partial y$), (e) the diffusivity coefficient K_{yy} and (f) the ratio $K_{yy}/|v^*|$ between the periods 1970-1990 and 2080-2100. The contour lines show the multi-model mean climatology of the first period of the respective quantity. Stippled regions show where the statistical significance of the difference is below the threshold 95%.

MRI

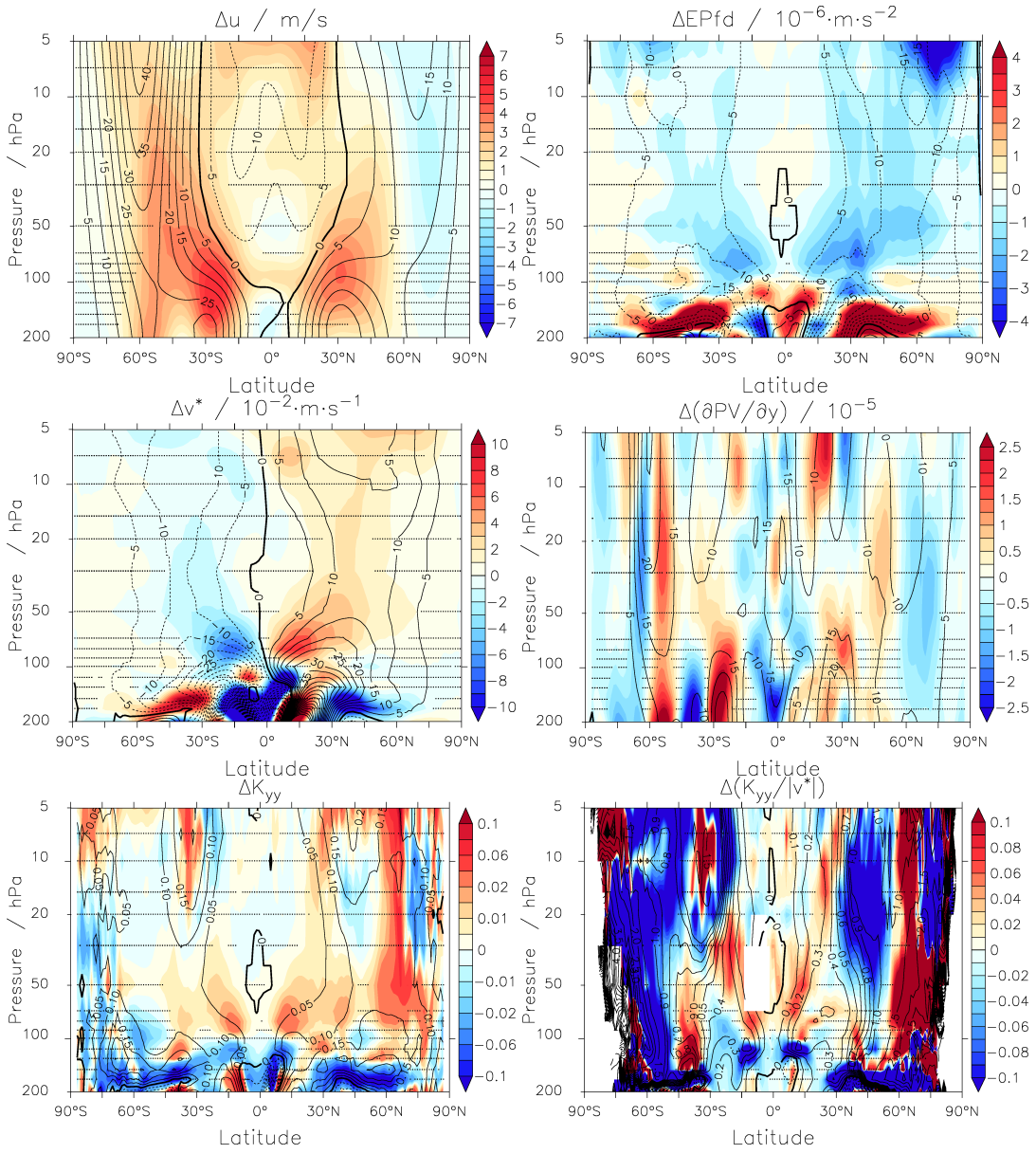

Figure 6. MRI CCMI REF-C2 model simulation differences (Δ) of (a) the zonal wind $\overline{u}$, (b) the EP flux divergence, (c) the meridonal residual circulation v*, (d) the meridional PV-gradient ($\partial PV/\partial y$), (e) the diffusivity coefficient K_{yy} and (f) the ratio $K_{yy}/|v^*|$ between the periods 1970-1990 and 2080-2100. The contour lines show the multi-model mean climatology of the first period of the respective quantity. Stippled regions show where the statistical significance of the difference is below the threshold 95%.

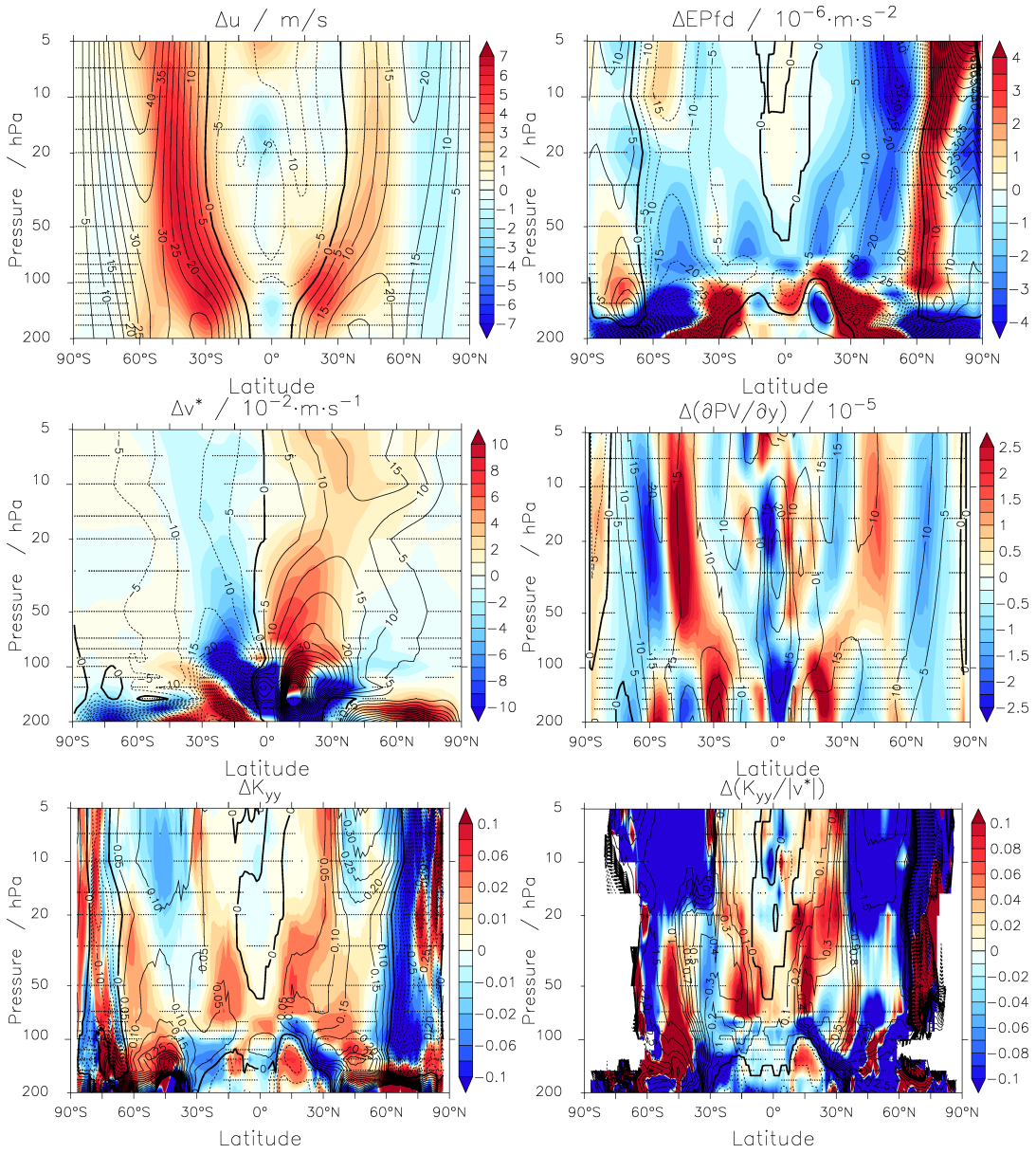

Figure 7. NIWA-UKCA CCMI REF-C2 model simulation differences (Δ) of (a) the zonal wind $\overline{u}$, (b) the EP flux divergence, (c) the meridonal residual circulation v*, (d) the meridional PV-gradient ($\partial PV/\partial y$), (e) the diffusivity coefficient K_{yy} and (f) the ratio $K_{yy}/|v^*|$ between the periods 1970-1990 and 2080-2100. The contour lines show the multi-model mean climatology of the first period of the respective quantity. Stippled regions show where the statistical significance of the difference is below the threshold 95%.

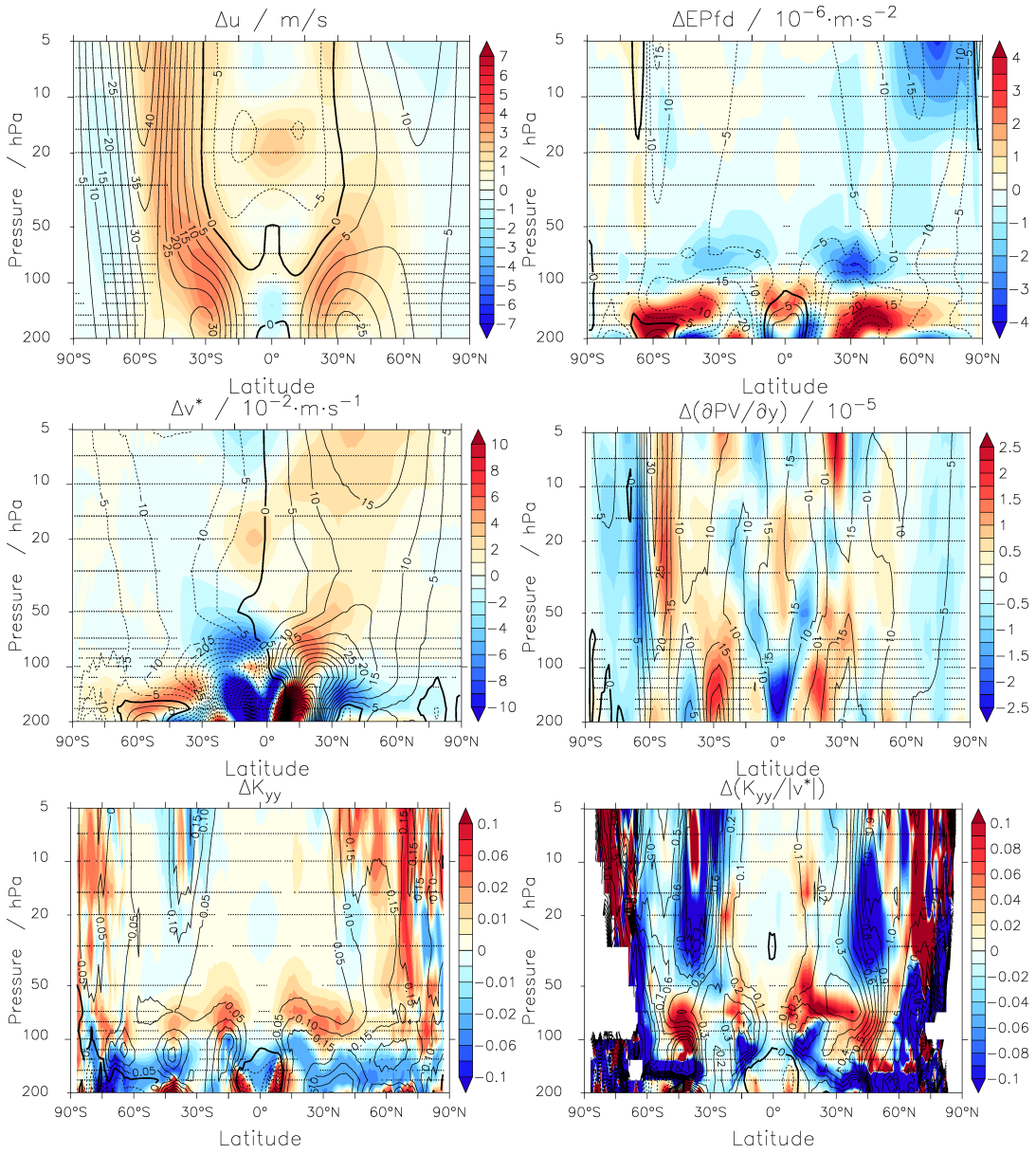

Figure 8. WACCM CCMI REF-C2 model simulation differences (Δ) of (a) the zonal wind $\overline{u}$, (b) the EP flux divergence, (c) the meridonal residual circulation v*, (d) the meridional PV-gradient ($\partial PV/\partial y$), (e) the diffusivity coefficient K_{yy} and (f) the ratio $K_{yy}/|v^*|$ between the periods 1970-1990 and 2080-2100. The contour lines show the multi-model mean climatology of the first period of the respective quantity. Stippled regions show where the statistical significance of the difference is below the threshold 95%.